Cortical centralspindlin and Gα have parallel roles in furrow initiation in early *C. elegans* embryos

Koen J. C. Verbrugghe[1,2] and John G. White[2,3,*]

[1]Laboratory of Genetics, [2]Laboratory of Molecular Biology and [3]Department of Anatomy, University of Wisconsin – Madison, Madison, WI 53706, USA

*Author for correspondence (e-mail: jwhite1@wisc.edu)

Accepted 15 March 2007
Journal of Cell Science 120, 1772-1778 Published by The Company of Biologists 2007
doi:10.1242/jcs.03447

Summary

Evidence from various systems suggests that either asters or the midzone of the mitotic spindle are the predominant determinants of cleavage plane position. Disrupting spindle midzone formation in the one-cell *Caenorhabditis elegans* embryo, such as by using mutants of the centralspindlin component ZEN-4, prevents completion of cytokinesis but does not inhibit furrowing. However, furrowing is inhibited by the simultaneous depletion of ZEN-4 with either PAR-2 or Gα, which are required for asymmetric divisions. Through studies of other genes required for the presence of an intact spindle midzone containing microtubule bundles, we found that furrowing failed in the absence of PAR-2 or Gα only when centralspindlin was absent from the furrow. We also found spindle length or microtubule distribution did not correlate with furrow initiation. We propose that centralspindlin acts redundantly with Gα to regulate furrow initiation.

Supplementary material available online at
http://jcs.biologists.org/cgi/content/full/120/10/1772/DC1

Key words: Cytokinesis, Spindle midzone, Centralspindlin, Furrow initiation

Introduction

Ingression of the cytokinetic furrow in animal cells is driven by the constriction of an actin-myosin ring (Glotzer, 2001; Mabuchi and Okuno, 1977). Numerous experiments implicate the mitotic apparatus as playing the key role in defining where the cytokinetic furrow will be positioned (Burgess and Chang, 2005; D'Avino et al., 2005; Rappaport, 1996). However, it is not clear which components of the mitotic apparatus provide the signals that initiate contractile ring assembly on the equator and activate contraction. In some cell types it appears that the asters play a dominant role in the initiation of furrowing, whereas in others it appears that the spindle midzone is dominant (Burgess and Chang, 2005; D'Avino et al., 2005). Studies of *Drosophila* and mammalian culture cells suggest that the spindle midzone has a major role in furrow formation in these cells (Cao and Wang, 1996; Gatti et al., 2000; Giansanti et al., 1998; Wheatley and Wang, 1996). By contrast, depletion or mutation of midzone components do not affect furrow initiation in the one-cell *Caenorhabditis elegans* embryo, but are required for the final separation of daughter cells after furrow ingression (Jantsch-Plunger et al., 2000; Powers et al., 1998; Raich et al., 1998; Schumacher et al., 1998). However, embryos depleted of both ZEN-4 (a kinesin required for midzone formation) and PAR-2 (required for establishing polarity during asymmetric divisions) fail to initiate furrowing (Dechant and Glotzer, 2003).

When polarity is disrupted during embryonic divisions of *C. elegans*, the length of the mitotic spindle is altered (Grill et al., 2001). Anaphase B spindle elongation is driven by cortical forces pulling on astral microtubules (Grill et al., 2001), in a mechanism that is regulated by the trimeric G-protein Gα (Colombo et al., 2003). Depletion of PAR-2, which localizes to the posterior cortex and acts upstream of Gα, or depletion of Gα itself decreases these forces and reduces spindle elongation when the midzone is disrupted but does not affect cytokinesis. However, depletion of Gα or PAR-2 together with ZEN-4 inhibits furrow formation (Dechant and Glotzer, 2003). From these and other observations it was argued that bundling of microtubules in the spindle midzone and spindle elongation act redundantly to decrease microtubule density at the equatorial cortex, and that this localized equatorial minimum induces furrowing (Dechant and Glotzer, 2003).

We have previously described the gene *spd-1*, which, when mutated or suppressed with RNA-mediated interference (RNAi), disrupts bundling of microtubules in, and the mechanical integrity of, the spindle midzone. However, the resultant lack of microtubule bundles does not give rise to cytokinesis defects in the one-cell embryo (Verbrugghe and White, 2004). *spd-1* encodes the *C. elegans* member of a family of spindle midzone-specific microtubule bundling proteins that includes mammalian PRC1, yeast Ase1p and plant MAP65 (Schuyler et al., 2003). We found that centralspindlin, a complex containing ZEN-4 and the GTPase activating protein (GAP) CYK-4 (Mishima et al., 2002), localizes near the ingressing cleavage furrow as well as the spindle midzone (see supplementary material Fig. S1). Furthermore, the furrow localization of centralspindlin is maintained in embryos depleted of SPD-1 but is not maintained in embryos depleted of other midzone components (Verbrugghe and White, 2004). These data suggest that the furrow localization of centralspindlin could allow completion of cytokinesis in the absence of the microtubule bundles (with their associated

Table 1. Quantification of the numbers of embryos that successfully initiate furrow ingression

	Wild type	*par-2*	*par-3*	*gpr-1/2*
Wild type		10/10	11/11	10/10
zen-4(or153)	10/10	0/10	29/31	1/11
cyk-4(RNAi)	10/10	1/10	10/10	ND
air-2(RNAi)	15/15	2/14	9/25	ND
spd-1(oj5)	10/10	16/16	11/11	10/10
car-1(RNAi)	10/10	12/12	10/10	ND
spd-1(oj5) zen-4(RNAi)	12/12	0/10	ND	ND
spd-1(oj5) cyk-4(RNAi)	10/10	1/11	ND	ND
spd-1(oj5) air-2(RNAi)	16/16	0/11	ND	ND

Number of embryos that furrow over the total number of embryos imaged. ND, not determined.

centralspindlin) in the spindle midzone (Verbrugghe and White, 2004). Because centralspindlin is detectable at the furrow early during furrowing (see supplementary material Fig. S1), we explored the possibility that this complex may have an additional role in furrow initiation.

Results

Bundled microtubules in the spindle midzone are not required for furrow initiation in the absence of *par-2* and Gα signaling

It has been suggested that the stimulus for furrowing is an equatorial region of reduced microtubule density that forms by the joint action of microtubule sequestration through bundling in the midzone and spindle elongation, which acts to move the asters away from the equator (Dechant and Glotzer, 2003). We explored this model by determining whether embryos depleted of various proteins required for bundling microtubules in the spindle midzone failed to furrow when depletion of PAR-2 compromised anaphase B spindle elongation. As expected from previous studies, we found that *zen-4(or153)* embryos (Severson et al., 2000) were able to initiate furrowing but *zen-4(or153) par-2(RNAi)* embryos were not (Table 1, Fig. 1E,F and supplementary material Movies 1, 2) (Dechant and Glotzer, 2003). Depletion of PAR-3, which localizes to the anterior cortex and restricts the localization of PAR-2, has a smaller effect on anaphase B spindle elongation (Grill et al., 2001), and *zen-4(or153)* embryos depleted of PAR-3 by RNAi were able to initiate furrowing most of the time (Table 1, Fig. 1G) (Dechant and Glotzer, 2003). Similar results were obtained when *cyk-4(RNAi)* was substituted for the mutant *zen-4(or153)* (see Table 1).

When we depleted AIR-2, a kinase that is part of the chromosomal kinetochore complex and has roles in both chromosome segregation and bundling microtubules in the spindle midzone (Schumacher et al., 1998), we obtained different results: *air-2(RNAi)* embryos furrow whereas most *air-2(RNAi) par-2(RNAi)* and *air-2(RNAi) par-3(RNAi)* embryos do not (Table 1). This is in accord with previous observations where the failure was attributed to reduced spindle elongation (Dechant and Glotzer, 2003). However, we found that *spd-1(oj5)*, *spd-1(oj5) par-2(RNAi)* and *spd-1(oj5) par-3(RNAi)* embryos were all able to furrow (Fig. 1I-K, Table 1 and supplementary material Movies 3, 4). Finally, we tested *car-1*, a gene encoding an RNA-associated protein that is required for the presence of microtubule bundles in the spindle midzone (Audhya et al., 2005; Squirrell et al., 2006). *car-1(RNAi)* embryos initiated furrowing, as did *car-1(RNAi) par-2(RNAi)* and *car-1(RNAi) par-3(RNAi)* embryos (Table 1). Given that the presence of microtubule bundles was severely disrupted in embryos lacking SPD-1 or CAR-1, these data indicate that the sequestration of microtubules by bundling in the midzone is not required for furrow initiation in the absence of PAR-2.

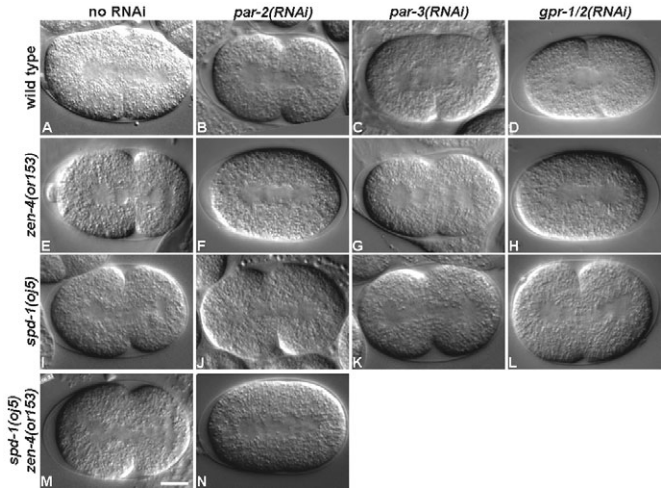

Fig. 1. Nomarski images of *C. elegans* embryos during cytokinesis showing furrow ingression or lack of furrowing. Furrowing fails in embryos mutant for *zen-4* and depleted of PAR-2 or GPR-1/2 but not in embryos mutant for *spd-1* and depleted of PAR-2 or GPR-1/2. Bar, 10 μm. We selected frames in which the furrow has reached the midzone or similar timepoints in embryos that failed to furrow.

It has been shown that depletion of the redundant Gα subunits *goa-1* and *gpa-16* prevents furrow initiation in *zen-4*-depleted embryos (Dechant and Glotzer, 2003). Gα signaling acts downstream of polarity and the PAR proteins to regulate cortical interactions with microtubules that mediate spindle rotation and elongation by modulating forces on astral microtubules (Gönczy and Rose, 2005). This suggests that it is the role of PAR-2 in regulating forces on astral microtubules (through Gα signaling) and not cell-fate specification that influences furrowing. We reduced Gα activity by simultaneously depleting GPR-1 and GPR-2, two nearly identical proteins that redundantly activate Gα (Colombo et al., 2003; Gotta et al., 2003). *gpr-1/2(RNAi)* had the same effect on furrow initiation as *par-2(RNAi)* and *goa-1(RNAi); gpa-16(RNAi)* (Dechant and Glotzer, 2003) because *zen-4(or153) gpr-1/2(RNAi)* embryos did not furrow whereas *spd-1(oj5) gpr-1/2(RNAi)* did (Table 1, Fig. 1D,H,L).

ZEN-4, CYK-4 and AIR-2 are all required to localize centralspindlin to the ingressing furrow; however, SPD-1 and CAR-1 are not (Squirrell et al., 1999; Verbrugghe and White, 2004). These observations suggest that it is centralspindlin localized to the furrow and not sequestration of microtubules by bundling in the spindle midzone that act to initiate furrow formation when PAR-2 or Gα signaling are depleted in the one-cell *C. elegans* embryo (see Table 2). However, an alternative explanation could be that because spindles elongate further in *spd-1(oj5)* embryos than in *zen-4(or153)* embryos (Verbrugghe

Table 2. Predictions and results to distinguish between two models for furrow ingression

Bundled MTs in spindle midzone	CS on furrow	Long spindle [e.g. *par-2*(+)]	Example	Prediction: spindle length model	Prediction: CS on furrow model	Actual
Yes	Yes	Yes	Wild type	+	+	+
Yes	Yes	No	*par-2*	+	+	+
No	Yes	Yes	*car-1*	+	+	+
No	Yes	No	*car-1 par-2*	–	+	+
No	No	Yes	*zen-4*	+	+	+
No	No	No	*zen-4 gpr-1/2*	–	–	–

In the first three columns, yes/no represents the presence (yes) or absence (no) of bundled microtubules (MTs) in the spindle midzone, centralspindlin (CS) on the furrow or long (yes) or short (no) spindles. In the last three columns, ± represents the ability to furrow. A spindle length model predicts that furrowing occurs in the absence of the microtubule bundles in the midzone when the spindle is long [i.e. >20 microns (Dechant and Glotzer, 2003)], and does not depend on the presence of CS on the furrow. However, our observations suggest a model that, in the absence of MTs in the midzone, furrowing depends on the presence of CS on the furrow and not spindle length.

and White, 2004), furrowing might occur in *spd-1(oj5) par-2(RNAi)* embryos because spindle elongation was not sufficiently suppressed.

Spindle length does not correlate with furrow initiation

To measure spindle elongation we repeated the combinatorial depletion experiments in strains expressing β-tubulin green fluorescent protein (GFP) (Strome et al., 2001). In order to analyze the distribution of microtubules at the cortex of live embryos, we used a multiphoton microscope (Wokosin et al., 2003) to collect images alternately at a plane near the middle of the embryo, to follow spindle elongation and cell cycle progression, and a plane near the surface, to view microtubule distribution at the cortex (Fig. 2A). *zen-4(or153)* embryos did not completely disrupt the appearance of microtubule bundles in the midzone, so we combined the mutant with RNAi suppression of ZEN-4 by feeding to give a stronger defect (data not shown). This treatment did not affect furrow initiation, as *zen-4(or153+RNAi)* embryos initiated furrowing (5/5) and *zen-4(or153+RNAi) par-2(RNAi)* embryos did not (0/5). We found that furrow initiation occurred significantly earlier in *spd-1(oj5)* embryos (40±20 seconds after the metaphase to anaphase transition, mean ± standard deviation) compared with wild-type [74±19.5 seconds (P<0.05) *t*-test with a one-tailed distribution] or other embryos lacking the bundled microtubules in the spindle midzone [76±18.2 seconds in *zen-4(or153+RNAi)* (P<0.01)], whereas depletion of *air-2* delayed furrow initiation [100±20 seconds (P<0.05) compared with wild-type or *zen-4*] (see supplementary material Fig. S2). In addition, depletion of PAR-2 [112±37.7 seconds for *par-2(RNAi)* and 90±10.0 seconds for *spd-1(oj5) par-2(RNAi)*] or GPR-1/2 [108±17.9 seconds for *gpr-1/2(RNAi)* and 106±11.4 seconds for *spd-1(oj5) gpr-1/2(RNAi)*] significantly delayed furrowing in embryos compared with wild type and *spd-1(oj5)* hermaphrodites (P<0.05 for each comparison).

We compared the length of the spindle at the time of furrowing in each embryo. In embryos that did not furrow we used the length of the spindle at 150 seconds after the metaphase to anaphase transition, at which time the spindle had reached equilibrium near its maximum length (see supplementary material Fig. S3). If furrow initiation is induced by an increase in spindle length, as has been suggested (Dechant and Glotzer, 2003), embryos that lack bundled microtubules in the spindle midzone and yet furrow should have spindle lengths above a threshold, whereas embryos that fail to induce furrows should have a spindle length below that threshold (see Table 2). Although we do not know the exact time that the signal to induce furrowing is generated, we measured spindle length at the time that furrow ingression first became apparent. This is a conservative estimate of the spindle length because if the relevant timepoint is earlier, the spindle will be shorter than our measured value and we will have erred on the side of favoring the spindle length model. Although the depletion of *par-2* and *gpr-1/2* did slow spindle elongation (see supplementary material Fig. S3), depleting these genes also delayed furrowing (see supplementary material Fig. S2). This meant that the length of the spindle at the time of furrow initiation was not always reduced as expected when *par-2* or *gpr-1/2* were depleted. We found that some cells had short spindles at the time of furrowing [17.4±2.6 microns in *spd-1(oj5)* and 17.1±0.7 microns in *spd-1(oj5) gpr-1/2(RNAi)*], whereas other embryos had long spindles but did not furrow {20.6±0.3 microns in *spd-1(oj5) zen-4(RNAi) par-2(RNAi)* [P<0.05 versus *spd-1(oj5)* and $P<10^{-4}$ versus *spd-1(oj5) gpr-1/2(RNAi)* *t*-test with a one-tailed distribution] and 21.8±3.5 microns in *spd-1(oj5) cyk-4(RNAi) par-2(RNAi)* [P<0.05 versus *spd-1(oj5)* and P<0.05 versus *spd-1(oj5) gpr-1/2(RNAi)*]} (Fig. 2B). Our data indicate that furrow initiation does not correlate with spindle length but rather correlates with the presence of centralspindlin near the equator. However, it is possible that separating the spindle poles even further could prevent furrow initiation (Rappaport, 1961).

Our observations suggest that, in the absence of bundled microtubules in the spindle midzone, there are two mechanisms for furrow initiation; one is dependent on centralspindlin localization near the furrow and the other is dependent on PAR-2 or Gα but not spindle length. This centralspindlin-independent mechanism does not involve spindle elongation. Embryos depleted of ZEN-4, CYK-4 or AIR-2 have no centralspindlin localized to the furrow (Verbrugghe and White, 2004) (see supplementary material Fig. S1). However, such embryos exhibit no difference in spindle length in cases that initiate furrowing [e.g. 20.1±1.1 microns in *air-2(RNAi)*] compared with those that do not [20.1±1.3 microns in *zen-4(RNAi) par-2(RNAi)* (P>0.4)] (Fig. 2).

There is no clear pattern of microtubule distribution at the cortex in live embryos

It is likely that microtubules have an important role in furrow initiation but it is not clear from the literature whether there is

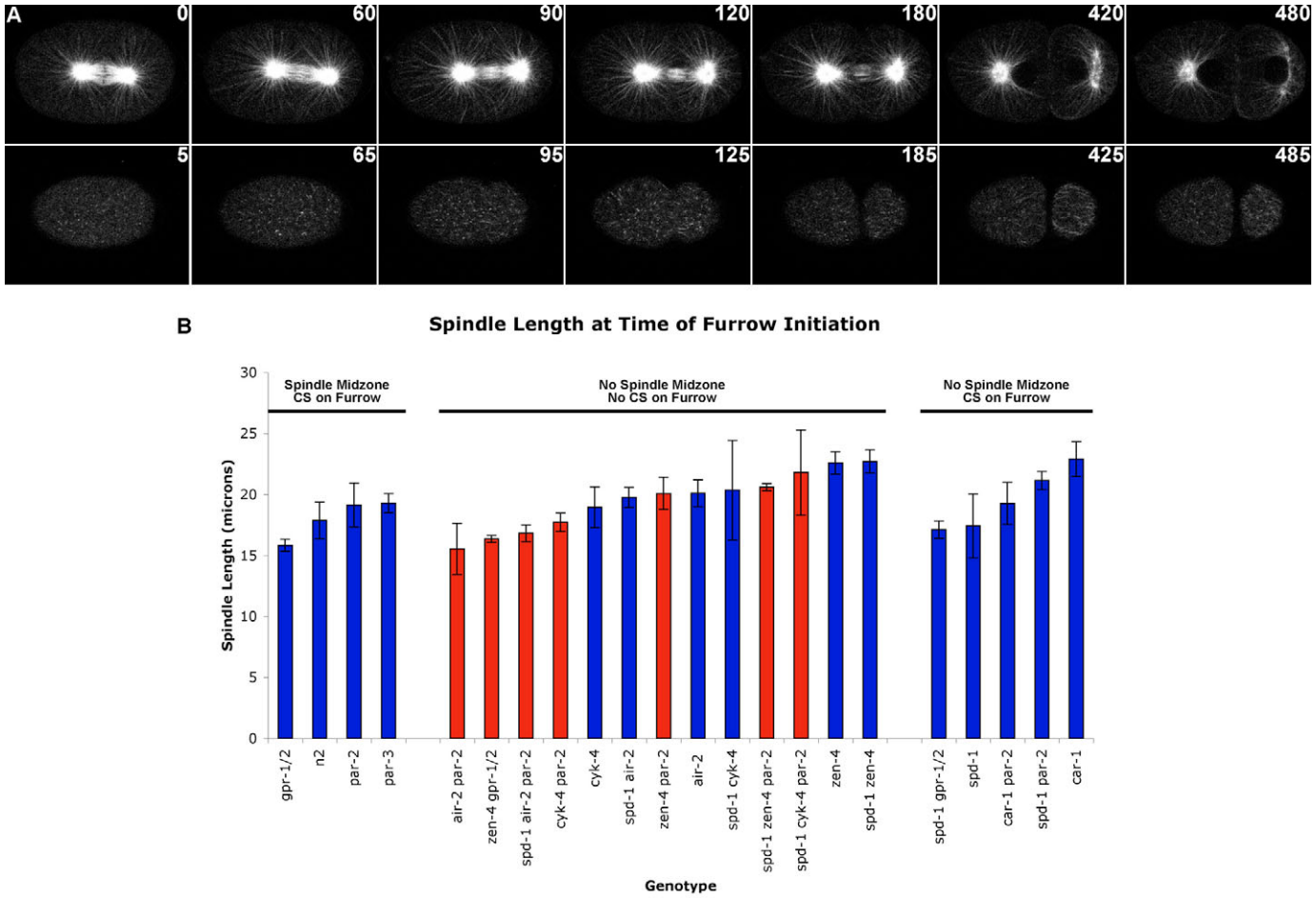

Fig. 2. Spindle length determination at the initiation of furrow ingression. (A) Time-lapse images of alternating mid- (top row) and cortical- (bottom row) planes of wild-type embryos expressing β-tubulin::GFP. Numbers represent time in seconds after the initiation of metaphase to anaphase transition. Bar, 10 μm. (B) Length of spindle at time of furrow ingression or 150 seconds after the metaphase to anaphase transition for embryos that fail to furrow (see text). Red bars represent embryos that fail to furrow. Blue bars are embryos that furrowed. Each bar represents the average length of the spindle in microns from five embryos and the error bars represent s.d. The bars are arranged by increasing spindle length.

a relative increase or decrease in microtubules at the cortex where the furrow will form, which we call the equatorial cortex. A decrease in microtubule density at the equatorial cortex in fixed *C. elegans* embryos was reported (Dechant and Glotzer, 2003). Disruption of microtubule bundling in the spindle midzone and depletion of *par-2* or Gα seemed to affect the microtubule distribution, and it was proposed that an increase in microtubule density at the equator explained the furrow defect. By contrast, a recent paper claims that in live embryos there is an increase in the amount of tubulin-GFP in the equator during contractile ring assembly, which occurs 20 seconds prior to furrow initiation (Motegi et al., 2006). In the light of these conflicting observations, we counted the number of microtubule ends at the cortical plane in live embryos and analyzed their distribution (Fig. 2A). We found no consistent difference in the number of microtubule ends in the equator compared with adjacent regions during or prior to furrow initiation (Fig. 3A) or a consistent change in the number of microtubules at the equator prior to initiation (Fig. 3B). We also did not find a consistent difference in microtubule distribution at the cortex in mutant *par-2*, *spd-1*, *spd-1 par-2* and *zen-4* embryos (Fig. 3C). Our data suggest that the distribution of microtubules at the cortex is unlikely to determine the position of contractile ring formation and furrow initiation.

Discussion

We found that depletion of SPD-1 and CAR-1 (two proteins required for bundling microtubules in the midzone but not for centralspindlin localization to the furrow) did not prevent furrow initiation in the absence of PAR-2 and Gα signalling, whereas disruption of the centraspindlin complex by depletion of ZEN-4, CYK-4 and AIR-2 did. Our data show that the presence of centralspindlin, but not spindle elongation or microtubule distribution at the cortex, correlates with furrow initiation in the absence of bundled microtubules in the spindle midzone. The localization of this complex of proteins to the furrow independently of the spindle midzone (Verbrugghe and White, 2004) supports the hypothesis that centralspindlin might have a role in furrow initiation.

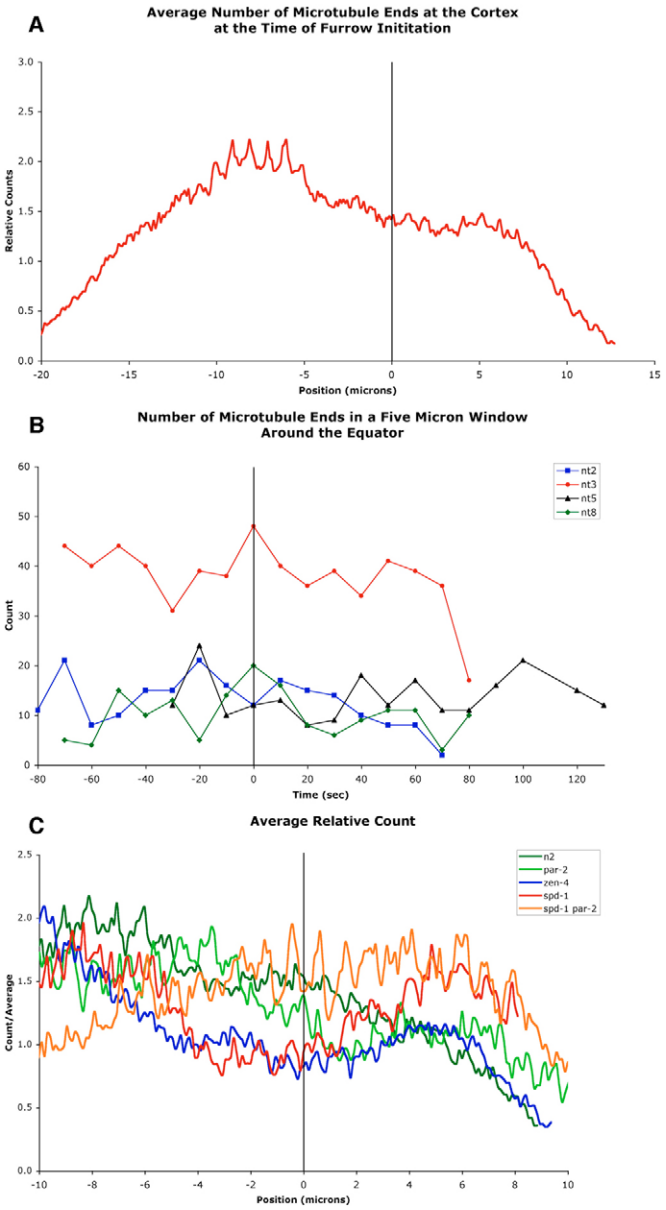

Fig. 3. Microtubule distribution at the cortex in live embryos. (A) Normalized number of microtubule ends along the length of the embryo at the time of furrow initiation. The number of microtubule ends in a 5 micron-wide window surrounding each position was divided by the mean of all of the values for that embryo in order to compare different embryos. Average of 10 embryos. 0 is the position where the furrow begins ingression, anterior is left (negative values) and posterior is right (positive values). There are valleys and peaks throughout the length of the embryo and yet the equatorial cortex does not align with the major minimum between the poles. Analysis of individual embryos indicates that the equatorial cortex sometimes aligns with a local maximum of microtubules and rarely aligns with the global minimum (see supplementary material Fig. S4). Similar results were obtained for all timepoints between the onset of anaphase and furrow initiation (see supplementary material Fig. S5). The steep decrease in microtubule ends is a consequence of the way in which microtubule ends are counted. The measurement windows have approximately the same lateral extent in the central region of the embryo, which is roughly cylindrical, and so the counts in this region are equivalent to microtubule density, but the area of cytoplasm fall-off in the poles, which gives rise to a reduction of microtubule end counts in these regions. See supplementary material Fig. S6 for analysis of this data using different window sizes. (B) Number of microtubule ends at the equatorial cortex before and after furrow initiation in four different wild-type embryos. Time 0 is when the furrow first appears. Each frame is 10 seconds apart. There is no consistent increase or decrease in the number of microtubule ends in the equatorial cortex at the time of furrow initiation or 20 seconds earlier when the contractile ring is expected to form. (C) Average relative number of microtubule ends around the equatorial cortex at the time of furrow initiation for various mutant combinations that can furrow. Each line is an average of three embryos. 0 is the position where the furrow begins ingression, anterior is left (negative values) and posterior is right (positive values). There is no consistent increase or decrease of microtubule ends at the equatorial cortex in embryos that furrow.

The RNAi and temperature-sensitive alleles used here, although consistent with the strongest phenotypes reported, are most likely not complete loss-of-function. The Dechant and Glotzer model proposes that sequestration of microtubules by bundling in the midzone and spindle elongation have a role in furrow ingression. Although the spindle midzone may not be completely disrupted in the experiments that we describe, we have clearly disrupted the vast majority of microtubule bundling and sequestration and yet have not managed to suppress furrow formation in conditions where centralspindlin is still present on the equatorial cortex.

One difficulty in determining whether a signal for cytokinesis originates from the asters or midzone is that the midzone is always placed between the two asters, and so the two putative signals will always initiate a furrow in the same place. To break this symmetry, laser ablation was used to sever the spindle between one pole and the midzone in *C. elegans* embryos (Bringmann and Hyman, 2005). It was found that two furrows formed, one at the midpoint between the spindle poles and one bisecting the midzone. Depletion of ZEN-4 eliminated the furrow bisecting the midzone and weakened the furrow bisecting the poles, whereas only the midzone-directed furrow was disrupted in *spd-1(oj5)* embryos (Bringmann and Hyman, 2005). This suggests that centralspindlin on the cortex might play a role in the aster-directed furrow. It would be intriguing to determine to which of the furrows ZEN-4::GFP localized in asymmetric spindle-severing assays, and whether depletion of *par-2* and Gα differentially affect these furrows. It has recently been proposed that LET-99 and the G-proteins are required for the aster-derived signal (Bringmann et al., 2007). The authors found that disruption of LET-99 and GPR-1/2 disrupted but did not completely block furrowing in *spd-1(oj5)* mutants and prevented furrow ingression in embryos in which the midzone was disrupted using laser ablation. Based on our data, this would suggest that laser ablation also disrupts localization of centralspindlin to the cortex.

Based on these data, we would like to propose the following model for furrow initiation in the *C. elegans* embryo (Fig. 4). As previously observed, the spindle midzone and asters act independently to induce furrow activity (Bringmann and Hyman, 2005). The mechanism by which the spindle midzone induces furrowing is unknown, but is not likely to involve differential microtubule densities at the cortex. Studies in other

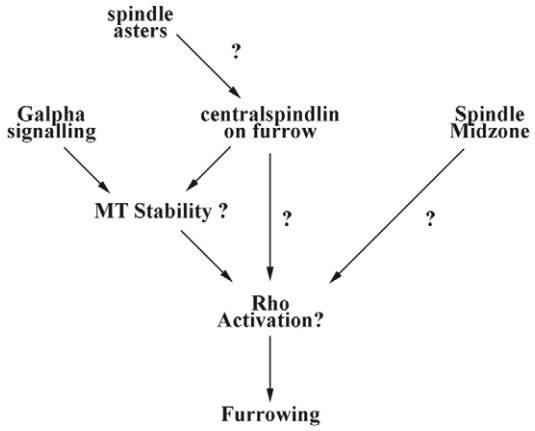

Fig. 4. Model for furrow initiation in the *C. elegans* one-cell embryo. We propose that the spindle midzone, centralspindlin on the cortex and Gα act in parallel to initiate furrowing. Although much of the mechanism is still poorly understood, it might act through microtubule stability and localized activation of Rho. See text for more details.

organisms have shown that CYK-4/MgcRacGAP at the midzone as well as the tips of microtubules near the equator bind to the RhoGEF Ect2 and this interaction is required for Rho localization and activation and cytokinesis (D'Avino et al., 2006; Nishimura and Yonemura, 2006; Somers and Saint, 2003; Yuce et al., 2005). This suggests a possible mechanism for furrow initiation in *C. elegans* as both LET-21, the *C. elegans* Ect2 homolog, and RHO-1, *C. elegans* RhoA, are required for furrow initiation (Jantsch-Plunger et al., 2000; Sonnichsen et al., 2005). However, it is not clear how a molecular signal generated in the midzone would travel to the cortex in the large *C. elegans* embryo. It is more plausible that centralspindlin at the cortex may recruit LET-21 to activate RHO-1 locally, indicating that the midzone plays some other, as yet unexplained, role. It is possible that astral microtubules direct centralspindlin to the cortex, as is observed in *Drosophila* (D'Avino et al., 2006; Inoue et al., 2004), although we do not observe centralspindlin associated with astral microtubules or moving in the cytoplasm towards the cortex. In addition to activating actin-myosin contractility by activating RHO-1, centralspindlin on the furrow could also bundle and stabilize microtubules. It has recently been suggested that stabilized or bundled microtubules are sufficient to induce furrowing (Alsop and Zhang, 2003; Canman et al., 2003; Inoue et al., 2004; Shannon et al., 2005), and at least one other midzone component, Survivin, has been shown to stabilize microtubules in mammalian cells (Mishima et al., 2002; Rosa et al., 2006). PAR-2 and Gα also appear to affect microtubule stability at the cortex in *C. elegans* (Labbe et al., 2003). This leads us to propose that microtubule stability, rather than distribution, may be important for furrow initiation in the *C. elegans* embryo and that PAR-2 (along with Gα) and centralspindlin act redundantly to stabilize microtubules at the equatorial cortex.

It is clear that cytokinesis is a robust and adaptable process with multiple redundant pathways to regulate furrow initiation, some of which are more or less important in certain cell types. Given the suggestions from this and other studies (Canman et al., 2003) that stabilized microtubules may be involved in defining the furrow region, it will be interesting to measure the residence times of microtubules at the equatorial cortex and to determine whether artificially stabilizing microtubules can induce furrowing in the absence of centralspindlin and PAR-2 or induce ectopic furrows in wild type in both *C. elegans* one-cell embryos and other cell types and organisms. It could also be informative to determine whether cortical flows (Bray and White, 1988) have a role in furrow initiation during cytokinesis, possibly by localizing centralspindlin or trimeric G protein regulators to the equator.

Materials and Methods

C. elegans strains and alleles

The Bristol strain N2 was used as the standard wild-type strain. The following additional strains were used: WH0109 [*unc-35(e259), spd-1(oj5)* I] (O'Connell et al., 1998), EU592 [*unc-8(n491sd), zen-4(or153ts)* IV] (Severson et al., 2000), WH0204 {*unc-119(ed3)* III; *ojIs1[beta-tubulin::GFP unc-119(+)]*} (Strome et al., 2001), WH0207 {*spd-1(oj5)* I; *ojIs1[beta-tubulin::GFP unc-119(+)]*} (Verbrugghe and White, 2004), WH0356 {*unc-8(n491sd), zen-4(or153ts)* IV; *ojIs1[beta-tubulin::GFP unc-119(+)]*} (this study), MGI70 {*zen-4(or153)* I; *xsEx6[zen-4:gfp]*} (Kaitna et al., 2000), and WH0279 {*unc-119(ed3)* III; *ojIs12[CYK-4::GFP unc-119(+)]*} (Verbrugghe and White, 2004). Culturing, handling and genetic manipulation of *C. elegans* was performed using standard procedures (Brenner, 1974). Temperature-sensitive strains were maintained at 16°C and L4 hermaphrodites shifted to 25°C for 16-24 hours before imaging.

RNAi

RNAi was performed by the feeding method (Timmons and Fire, 1998). For *par-2*, *par-3* and *gpr-1/2*, feeding vectors were constructed by inserting the appropriate cDNA clone into plasmid L4440. This plasmid was then transformed into the bacterial strain HT115(DE3). Feeding vectors for *zen-4*, *air-2* and *cyk-4* were reported earlier (Verbrugghe and White, 2004). The cDNA clones used were as follows: yk325e4 (for pR*par-2*), yk552e12 (pR*par-3*) and yk645d1 (pR*gpr-1*). *gpr-1* and *gpr-2* are >97% identical at the RNA level and so both genes are downregulated by double-stranded RNA (dsRNA) to *gpr-1* (Gotta et al., 2003). The RNAi feeding vector for *car-1* and *act-2* was obtained from the chromosome I library built by the Ahringer laboratory (Fraser et al., 2000). Individual colonies were grown overnight in 5 ml LB+ampicilin and then seeded on RNAi plates that were allowed to dry and induce RNA for at least one day. L4 hermaphrodites were allowed to feed for ⩾24 hours before analysis (Timmons and Fire, 1998). Hermaphrodites were allowed to feed on *car-1* RNAi bacteria for ⩾30 hours and *gpr-1/2* RNAi bacteria for ⩾52 hours to get a stronger phenotype. Temperature-sensitive strains were first grown at 16°C and then shifted to 25°C for 18-24 hours on these plates before imaging. For double RNAi experiments bacteria cultures were separately grown overnight and then mixed in equal volumes before seeding.

Live imaging

For all imaging two or three hermaphrodites were placed in a drop of M9 or egg buffer on a coverslip, and cut with a small scalpel perpendicular to the anterior-posterior axis at the midline in order to release embryos. The slide containing an agar pad was lowered onto the coverslip, and the agar pad was trimmed and the slide sealed with molten Vaseline. All recordings were performed at 25°C. Temperature was controlled through the room thermostat or locally, using a hair dryer equipped with a feedback thermocouple to heat the microscope stage. Nomarski imaging was performed using the four-dimensional (4D)-imaging microscopy described previously (Thomas and White, 1998). We used a Nikon Optiphot-2 upright microscope with a Nikon PlanApo 100× 1.4 NA DIC or 60× 1.4 NA DIC lens and a Hamamatsu C2400 CCD camera or a Nikon Diaphot300 inverted microscope with a 60× 1.4 NA DIC lens and a Sony XC-75 CCD camera. All of the images in Fig. 1 were obtained with the upright microscope and the 100× lens. All GFP imaging was performed using multiphoton excitation using an optical workstation (Wokosin et al., 2003) that consisted of a Nikon Eclipse TE300DV inverted microscope with a Nikon Super Fluor 100× 1.3 NA lens. The excitation source was a Ti:sapphire laser tuned to 890 nm. The detector was a high quantum efficiency Hamamatsu H7422-40 detector (Hamamatsu Photonics, Hamamatsu City, Japan). To determine microtubule distribution at the cortex, we alternated between imaging a cortical plane and a plane in the middle of the embryo in order to follow the cell cycle using spindle morphology. To pick a cortical plane we used the focusing motor to find the plane where background cytoplasmic signal disappeared and moved back 2 microns.

Data analysis

4D Nomarski movies were analyzed using 4D Viewer (Thomas and White, 1998),

multiphoton movies were analyzed using ImageJ (http://rsb.info.nih.gov/ij/) and figures were prepared using Adobe Photoshop (Adobe Systems, San Jose, CA). Image manipulations consisted of adjustment of brightness and contrast and were applied to the whole image. Each image from a time series was adjusted in the same way. We used the line tool of ImageJ to measure spindle length by measuring from the center of the anterior aster to the center of the posterior aster. All measurements of time and length were reported as mean ± s.d. from five embryos. To measure microtubule distribution at the cortex in a series of timepoints, we used the smoothing function to reduce noise and set a threshold so as to mark the bright tubulin-GFP spot signals but not the smaller noise. We wrote a macro (available on request) to automate counting of the number of spots, using the analyze particles function. Briefly, a box was drawn around the embryo and the macro used the dimension of the box to draw a smaller box of the same height but 10 pixels (~1 micron) wide. The number of particles in this box was counted for each frame of the time series and then the box was moved right one pixel. This was repeated until the whole region was covered. The numerical output was analyzed using Microsoft Excel (Microsoft, Redmond, WA). To compare different embryos, we normalized each value by dividing the measured value by the mean of all of the values for that embryo. To analyze the data using different sized windows, we averaged the data from non-overlapping windows that cover the desired width.

We would like to thank Jasmine Parvaz and Jayne Squirrell as well as the other members of the White Laboratory for discussion and comments on the manuscript. We are grateful to Yuji Kohara for cDNA clones. This work was supported by a grant from the National Institutes of Health (NIH) (RO1 GM7583) to J.W. K.V. was supported in part by an NIH predoctoral training grant (5T32 GM07133) to the Laboratory of Genetics.

References

Alsop, G. B. and Zhang, D. (2003). Microtubules are the only structural constituent of the spindle apparatus required for induction of cell cleavage. *J. Cell Biol.* **162**, 383-390.

Audhya, A., Hyndman, F., McLeod, I. X., Maddox, A. S., Yates, J. R., 3rd, Desai, A. and Oegema, K. (2005). A complex containing the Sm protein CAR-1 and the RNA helicase CGH-1 is required for embryonic cytokinesis in Caenorhabditis elegans. *J. Cell Biol.* **171**, 267-279.

Bray, D. and White, J. G. (1988). Cortical flow in animal cells. *Science* **239**, 883-888.

Brenner, S. (1974). The genetics of Caenorhabditis elegans. *Genetics* **77**, 71-94.

Bringmann, H. and Hyman, A. A. (2005). A cytokinesis furrow is positioned by two consecutive signals. *Nature* **436**, 731-734.

Bringmann, H., Cowan, C. R., Kong, J. and Hyman, A. A. (2007). LET-99, GOA-1/GPA-16, and GPR-1/2 are required for aster-positioned cytokinesis. *Curr. Biol.* **17**, 185-191.

Burgess, D. R. and Chang, F. (2005). Site selection for the cleavage furrow at cytokinesis. *Trends Cell Biol.* **15**, 156-162.

Canman, J. C., Cameron, L. A., Maddox, P. S., Straight, A., Tirnauer, J. S., Mitchison, T. J., Fang, G., Kapoor, T. M. and Salmon, E. D. (2003). Determining the position of the cell division plane. *Nature* **424**, 1074-1078.

Cao, L. G. and Wang, Y. L. (1996). Signals from the spindle midzone are required for the stimulation of cytokinesis in cultured epithelial cells. *Mol. Biol. Cell* **7**, 225-232.

Colombo, K., Grill, S. W., Kimple, R. J., Willard, F. S., Siderovski, D. P. and Gonczy, P. (2003). Translation of polarity cues into asymmetric spindle positioning in Caenorhabditis elegans embryos. *Science* **300**, 1957-1961.

D'Avino, P. P., Savoian, M. S. and Glover, D. M. (2005). Cleavage furrow formation and ingression during animal cytokinesis: a microtubule legacy. *J. Cell Sci.* **118**, 1549-1558.

D'Avino, P. P., Savoian, M. S., Capalbo, L. and Glover, D. M. (2006). RacGAP50C is sufficient to signal cleavage furrow formation during cytokinesis. *J. Cell Sci.* **119**, 4402-4408.

Dechant, R. and Glotzer, M. (2003). Centrosome separation and central spindle assembly act in redundant pathways that regulate microtubule density and trigger cleavage furrow formation. *Dev. Cell* **4**, 333-344.

Fraser, A. G., Kamath, R. S., Zipperlen, P., Martinez-Campos, M., Sohrmann, M. and Ahringer, J. (2000). Functional genomic analysis of C. elegans chromosome I by systematic RNA interference. *Nature* **408**, 325-330.

Gatti, M., Giansanti, M. G. and Bonaccorsi, S. (2000). Relationships between the central spindle and the contractile ring during cytokinesis in animal cells. *Microsc. Res. Tech.* **49**, 202-208.

Giansanti, M. G., Bonaccorsi, S., Williams, B., Williams, E. V., Santolamazza, C., Goldberg, M. L. and Gatti, M. (1998). Cooperative interactions between the central spindle and the contractile ring during Drosophila cytokinesis. *Genes Dev.* **12**, 396-410.

Glotzer, M. (2001). Animal cell cytokinesis. *Annu. Rev. Cell Dev. Biol.* **17**, 351-386.

Gönczy, P. and Rose, L. S. (2005). Asymmetric cell division and axis formation in the embryo. In *WormBook* (ed. The *C. elegans* Research Community), WormBook, doi/10.1895/wormbook.1.30.1, http://www.wormbook.org.

Gotta, M., Dong, Y., Peterson, Y. K., Lanier, S. M. and Ahringer, J. (2003). Asymmetrically distributed C. elegans homologs of AGS3/PINS control spindle position in the early embryo. *Curr. Biol.* **13**, 1029-1037.

Grill, S. W., Gonczy, P., Stelzer, E. H. and Hyman, A. A. (2001). Polarity controls forces governing asymmetric spindle positioning in the Caenorhabditis elegans embryo. *Nature* **409**, 630-633.

Inoue, Y. H., Savoian, M. S., Suzuki, T., Mathe, E., Yamamoto, M. T. and Glover, D. M. (2004). Mutations in orbit/mast reveal that the central spindle is comprised of two microtubule populations, those that initiate cleavage and those that propagate furrow ingression. *J. Cell Biol.* **166**, 49-60.

Jantsch-Plunger, V., Gonczy, P., Romano, A., Schnabel, H., Hamill, D., Schnabel, R., Hyman, A. A. and Glotzer, M. (2000). CYK-4: A Rho family gtpase activating protein (GAP) required for central spindle formation and cytokinesis. *J. Cell Biol.* **149**, 1391-1404.

Kaitna, S., Mendoza, M., Jantsch-Plunger, V. and Glotzer, M. (2000). Incenp and an aurora-like kinase form a complex essential for chromosome segregation and efficient completion of cytokinesis. *Curr. Biol.* **10**, 1172-1181.

Labbe, J. C., Maddox, P. S., Salmon, E. D. and Goldstein, B. (2003). PAR proteins regulate microtubule dynamics at the cell cortex in C. elegans. *Curr. Biol.* **13**, 707-714.

Mabuchi, I. and Okuno, M. (1977). The effect of myosin antibody on the division of starfish blastomeres. *J. Cell Biol.* **74**, 251-263.

Mishima, M., Kaitna, S. and Glotzer, M. (2002). Central spindle assembly and cytokinesis require a kinesin-like protein/RhoGAP complex with microtubule bundling activity. *Dev. Cell* **2**, 41-54.

Motegi, F., Velarde, N. V., Piano, F. and Sugimoto, A. (2006). Two phases of astral microtubule activity during cytokinesis in C. elegans embryos. *Dev. Cell* **10**, 509-520.

Nishimura, Y. and Yonemura, S. (2006). Centralspindlin regulates ECT2 and RhoA accumulation at the equatorial cortex during cytokinesis. *J. Cell Sci.* **119**, 104-114.

O'Connell, K. F., Leys, C. M. and White, J. G. (1998). A genetic screen for temperature-sensitive cell-division mutants of Caenorhabditis elegans. *Genetics* **149**, 1303-1321.

Powers, J., Bossinger, O., Rose, D., Strome, S. and Saxton, W. (1998). A nematode kinesin required for cleavage furrow advancement. *Curr. Biol.* **8**, 1133-1136.

Raich, W. B., Moran, A. N., Rothman, J. H. and Hardin, J. (1998). Cytokinesis and midzone microtubule organization in Caenorhabditis elegans require the kinesin-like protein ZEN-4. *Mol. Biol. Cell* **9**, 2037-2049.

Rappaport, R. (1961). Experiments concerning the cleavage stimulus in sand dollar eggs. *J. Exp. Zool.* **148**, 81-89.

Rappaport, R. (1996). *Cytokinesis in Animal Cells*. New York: Cambridge University Press.

Rosa, J., Canovas, P., Islam, A., Altieri, D. C. and Doxsey, S. J. (2006). Survivin modulates microtubule dynamics and nucleation throughout the cell cycle. *Mol. Biol. Cell* **17**, 1483-1493.

Schumacher, J. M., Golden, A. and Donovan, P. J. (1998). AIR-2: an Aurora/Ipl1-related protein kinase associated with chromosomes and midbody microtubules is required for polar body extrusion and cytokinesis in Caenorhabditis elegans embryos. *J. Cell Biol.* **143**, 1635-1646.

Schuyler, S. C., Liu, J. Y. and Pellman, D. (2003). The molecular function of Ase1p: evidence for a MAP-dependent midzone-specific spindle matrix. *J. Cell Biol.* **160**, 517-528.

Severson, A. F., Hamill, D. R., Carter, J. C., Schumacher, J. and Bowerman, B. (2000). The aurora-related kinase AIR-2 recruits ZEN-4/CeMKLP1 to the mitotic spindle at metaphase and is required for cytokinesis. *Curr. Biol.* **10**, 1162-1171.

Shannon, K. B., Canman, J. C., Moree, C. B., Tirnauer, J. S. and Salmon, E. D. (2005). Taxol-stabilized microtubules can position the cytokinetic furrow in mammalian cells. *Mol. Biol. Cell* **16**, 4423-4436.

Somers, W. G. and Saint, R. (2003). A RhoGEF and Rho family GTPase-activating protein complex links the contractile ring to cortical microtubules at the onset of cytokinesis. *Dev. Cell* **4**, 29-39.

Sonnichsen, B., Koski, L. B., Walsh, A., Marschall, P., Neumann, B., Brehm, M., Alleaume, A. M., Artelt, J., Bettencourt, P., Cassin, E. et al. (2005). Full-genome RNAi profiling of early embryogenesis in Caenorhabditis elegans. *Nature* **434**, 462-469.

Squirrell, J. M., Wokosin, D. L., White, J. G. and Bavister, B. D. (1999). Long-term two-photon fluorescence imaging of mammalian embryos without compromising viability. *Nat. Biotechnol.* **17**, 763-767.

Squirrell, J. M., Eggers, Z. T., Luedke, N., Saari, B., Grimson, A., Lyons, G. E., Anderson, P. and White, J. G. (2006). CAR-1, a protein that localizes with the mRNA decapping component DCAP-1, is required for cytokinesis and ER organization in Caenorhabditis elegans embryos. *Mol. Biol. Cell* **17**, 336-344.

Strome, S., Powers, J., Dunn, M., Reese, K., Malone, C. J., White, J., Seydoux, G. and Saxton, W. (2001). Spindle dynamics and the role of gamma-tubulin in early Caenorhabditis elegans embryos. *Mol. Biol. Cell* **12**, 1751-1764.

Thomas, C. F. and White, J. G. (1998). Four-dimensional imaging: the exploration of space and time. *Trends Biotechnol.* **16**, 175-182.

Timmons, L. and Fire, A. (1998). Specific interference by ingested dsRNA. *Nature* **395**, 854.

Verbrugghe, K. J. and White, J. G. (2004). SPD-1 is required for the formation of the spindle midzone but is not essential for the completion of cytokinesis in C. elegans embryos. *Curr. Biol.* **14**, 1755-1760.

Wheatley, S. P. and Wang, Y. (1996). Midzone microtubule bundles are continuously required for cytokinesis in cultured epithelial cells. *J. Cell Biol.* **135**, 981-989.

Wokosin, D. L., Squirrell, J. M., Eliceiri, K. W. and White, J. G. (2003). Optical workstation with concurrent, independent multiphoton imaging and experimental laser microbeam capabilities. *Rev. Sci. Instrum.* **74**, 1-9.

Yuce, O., Piekny, A. and Glotzer, M. (2005). An ECT2-centralspindlin complex regulates the localization and function of RhoA. *J. Cell Biol.* **170**, 571-582.